Available online at www.sciencedirect.com

ScienceDirect

journal homepage: www.jfda-online.com

Original Article

A low cost smart system to analyze different types of edible Bird's nest adulteration based on colorimetric sensor array

*Xiaowei Huang, Zhihua Li**, Xiaobo Zou*, Jiyong Shi, Haroon Elrasheid Tahir, Yiwei Xu, Xiaodong Zhai, Xuetao Hu*

School of Agricultural Equipment Engineering, School of Food and Biological Engineering, Jiangsu University, 301 Xuefu Rd., 212013, Zhenjiang, Jiangsu, China

ARTICLE INFO

Article history:
Received 7 April 2019
Received in revised form
19 June 2019
Accepted 24 June 2019
Available online 16 July 2019

Keywords:
Colorimetric sensor array
Edible bird's nest
Adulteration
Multi-layered network model
Smart system

ABSTRACT

This study was performed to develop a low-cost smart system for identification and quantification of adulterated edible bird's nest (EBN). The smart system was constructed with a colorimetric sensor array (CSA), a smartphone and a multi-layered network model. The CSA were used to collect the odor character of EBN and the response signals of CSA were captured by the smartphone systems. The principal component analysis (PCA) and hierarchical cluster analysis (HAC) were used to inquiry the similarity among authentic and adulterated EBNs. The multi-layered network model was constructed to analyze EBN adulteration. In this model, discrimination of authentic EBN and adulterated EBN was realized using back-propagation neural networks (BPNN) algorithm. Then, another BPNN-based model was developed to identify the type of adulterant in the mixed EBN. Finally, adulterated percentage prediction model for each kind of adulterate EBN was built using partial least square (PLS) method. Results showed that recognition rates of the authentic EBN and adulterated EBN was as high as 90%. The correlation coefficient of percentage prediction model for calibration set was 0.886, and 0.869 for prediction set. The low-cost smart system provides a real-time, nondestructive tool to authenticate EBN for customers and retailers.

1. Introduction

Edible bird's nest (EBN) ('Yanwo' in mandarin) is produced from the saliva of swiftlets (Aves: Apodidae), which has been esteemed a naturally nutritious food by Chinese since the Tang dynasty (618 AD) [1–3]. Due to the abundant nutritional value (water-soluble protein, carbohydrate, iron, inorganic salt and fiber), EBN was regarded as a precious medicinal food

* *Corresponding author.*
** *Corresponding author.*
E-mail addresses: lizh@ujs.edu.cn (Z. Li), zou_xiaobo@ujs.edu.cn (X. Zou).
https://doi.org/10.1016/j.jfda.2019.06.004

not only in Asia, also warmly welcomed by Western countries [4–8]. However, it is a tough process to gather EBN from the wild, which totally depends on dangerous manual work. As a result, EBN is sold at a high price and exposed to the adulteration problems. The adulterants usually found in EBN were high-protein substances including egg white [4] and porcine skin [9], high-carbohydrate substances including *tremella* fungus [1] and agar [3]. These adulterants were clandestinely added to increase EBNs' net weight. Although the adulteration would not harm human health directly, it severely impaired market competition and consumer's interests. Therefore, it is necessary to establish appropriate methods to identify the adulteration.

At present, several analytical approaches have been successfully used to detect the EBN adulterants, such as polymerase chain reaction (PCR) [1,9], immunoblotting assay [10], gas chromatography–mass spectrometry (GC–MS) [10,11], Raman spectra technique [12] and anti-peptide polyclonal antibody [13] and nutritional profile analysis [4]. These approaches show advantages as high-accuracy and high-stability, but expensive instruments, time-consuming preparation and highly skilled operators are required. Fourier transform infrared spectroscopy (FTIR) [6,14] can achieve rapid and nondestructive distinguishment of EBN geographic origins. However, it is difficult to discriminate pure EBN from adulteration using FTIR because the adulterants are usually of high-content of protein and carbohydrate. It is also very difficult to predict the mixing ratio of adulterants by FTIR. Therefore, a suitable method to identify and quantify the adulterants in EBN is urgently needed.

The major components of EBN include amino acids, carbohydrate, Sialic acid, inorganic salt et.al. The type and proportion of these components constitute the characteristic volatile components (VCs) in EBN. Similarly, adulterants also own unique natural and characteristic VCs. The analysis of VCs is a reasonable thinking for identification of authentic and adulterated EBN.

Colorimetric sensor array is a VC-sensing device based on multiple cross-responsive sensor elements [15]. The chemo-responsive elements can change color in either reflected or absorbed light depending on the changes in chemical environment [16]. It aims to mimic the mammalian olfactory system by producing composite, but unique responses when exposed to the detected objects. Compared with some common VC detecting methods (GC-MS and electronic nose) [17], the colorimetric sensor array showed advantages as rapid and non-destructive. It can avoid the side effects of humidity, which has emerged as a powerful tool for detection of food quality [18–20]. Colorimetric sensor array has been applied to identification of food adulteration such as fruit pickle [21], whiskeys [22,23], fruit juice [24]. However, several problems are still waiting to extend its widely application out of the laboratory, the main one is the lack of portable and intelligent device for colorimetric sensor array [16]. Fortunately, smartphone has become an essential device in our daily lives during the past years, which could be combined with colorimetric sensor array to overcome these defects.

In this research, a colorimetric sensor array was designed to identify four types of adulterated EBN. A self-developed smart cellphone system was used to capture and process the sensor response signal. Meanwhile, a multi-layered network model was designed to identify the pure and adulterated EBN. Then, back-propagation neural network (BPNN) algorithm was employed to distinguish the adulterant type of samples. At last, partial least square (PLS) algorithm was used to determine the percentage of adulterants.

2. Materials and methods

2.1. Sample preparation

The EBN samples from Indonesia and Malaysia were supplied by Chinese Academy of Inspection and Quarantine. Other adulterate materials including egg, porcine skin and *tremella* fungus were purchased from the local market. Agar was purchased from Sinopharm Chemical Reagent Co., Ltd (Shanghai, China).

For qualitative and quantitative detection, the mixtures of the pure EBN with the adulterants mentioned above were prepared. The mixed proportions of each adulterant ranged from 10% to 75% (w/w). 800 EBN mixture samples including 200 egg white adulterated samples (10%, 20%, 50% and 75%), 200 porcine skin adulterated samples (10%, 20%, 50% and 75%), 200 *tremella* fungus adulterated samples (10%, 20%, 50% and 75%), 200 agar adulterated samples (10%, 20%, 50% and 75%) were prepared. At the same time, 50 pure EBN samples, 50 pure egg white samples, 50 pure porcine skin samples, 50 pure *tremella* fungus and 50 pure agar samples were also prepared. The total sample number was 1050. The weight of each sample was 200 mg. All solid samples were packed with PVC bag and stored at 4 °C before analysis.

2.2. Determination of nutritional components

The protein, carbohydrate and Sialic acid were the main nutritional components of EBN. The protein concentration was determined using the classical kjeldahl method. Microwave Digestion System (MDS-15, Sineo microwave chemistry technology Co. LTD, Shanghai, China) was used to digest samples. The BUCHI's automated Kjeldahl system (KjelMaster K-375, BUCHI, Shanghai) was used to detect the nitrogen content. Titrate the contents of the receiver flask with sodium hydroxide solution (0.1 mol/L) to neutral endpoint [10,25]. Record the volume of hydroxide required. The total protein is calculated by the following formula:

$$\text{Protein contents (\%)} = (V_{\text{HCl/mL of sample}} - V_{\text{HCl /mL of blank}}) \times N_{\text{HCl}} \times 0.14 \times 6.25 / \text{Sample weight in gram} \quad (1)$$

Total carbohydrate content was calculated by the following formula:

$$\text{Total carbohydrates contents (\%)} = 100\text{-(weight in grams [protein + water + ash] in 100 g of sample)} \quad (2)$$

The Sialic acid content was measured using the high-performance liquid chromatography (HPLC). This experimentation was carried out by using a Shimadzu HPLC system. The mobile phase eluted using 7% (v/v) methanol, 9% (v/v)

acetonitrile in water for 40 min. The elution speed was 1 mL/min isocratic elution. The detection wavelength was at 230 nm Neu5Ac standard solution was prepared at 0.1, 1, 5, 10, 25, 50, 100, 200, 400, 750, 1000 μg/mL. All injections were kept at 35 °C.

2.3. Volatile component detection

Gas chromatographic method was used to analyze the characteristic VCs of pure EBN and adulterants. The characteristic VCs represent major difference between adulterants and pure EBN. It could be used to guide the selection of chemoresponsive dyes. Chromatography was performed on an Agilent 6890 gas chromatography (Santa Clara, CA, USA) equipped with a 5973 N mass selective detector. Separation was achieved using a DB-5MS capillary column (i.d., 30 m × 0.25 mm; film thickness, 0.25 μm). Sample (500 mg) were placed in a 20 mL vial and the vial was then tightly capped with PTFE/silicone septum. A manual solid phase microextraction (SPME) holder (Supelco, Bellefonte, PA) with a divinylbenzene/carboxen/polydimethylsiloxane (DVB/CAR/PDMS, 50/30 lm, coating 1 cm) fiber (Supelco) was used to extract headspace volatiles from samples. GC-MS temperatures were as following: injector, 250 °C; column, 300 °C with an increment of 10 °C/min; transfer line, 250 °C; ion source, 200 °C; and quadrupole temperature, 150 °C. Ionization was achieved with a 70 eV electron beam and an electron multiplier voltage of 350 V. The mass spectrometer was programmed under electron impact (EI) in a full scan mode at *m/z* 50–550 with a scanning rate of a 2 scans/s [11].

2.4. Application of the smart system for EBN detection

2.4.1. Fabrication of colorimetric sensor array

The colorimetric sensor arrays were fabricated using the classical method described in Ref. [15]. Firstly, optimization of chemoresponse dyes was performed according to the GC-MS results. The selected chemoresponse dyes should be sensitive to the characteristic VCs of adulterants and pure EBN. Eventually, 10 pH indicators and 6 porphyrins materials were selected. Then each dye solution (1 mM) was spotted on the silica gel plate (Merck KGaA, Darmstadt, Germany) using 0.1 μL microcapillary tubes. Then the arrays were stored in a nitrogen-flushed valve bag before further usage. The 16 dyes are as following:

(1) Bromocresol green
(2) Methylene blue
(3) Bromophenol blue
(4) Bromocresol purple
(5) Methyl red
(6) Neutral red
(7) Thymol blue
(8) 5,10,15,20-Tetraphenyl-21 h, 23 h-Porphine Cobalt(Ii)
(9) 5,10,15,20-Tetraphenyl-21H, 23H-porphine manganese(III) chloride
(10) 2,3,7,8,12,13,17,18-Octaethyl-21H, 23H-porphine manganese(III) chloride
(11) 5,10,15,20-Tetraphenylporphyrin
(12) 5,10,15,20-Tetraphenyl-21 h, 23 h-Porphine Copper
(13) 2,3,9,10,16,17,23,24-octakis(octyloxy)-29H, 31H-phthalocyanine
(14) 5,10,15,20tetrakis(Pentafluorophenyl)Porphyriniron(Iii) Chloridecomplex
(15) 5,10,15,20-Tetraphenyl-21 h, 23 h-Porphine Iron(Iii) Chloride
(16) 5,10,15,20-Tetraphenylporphyrinato Zinc

2.4.2. Construction of smart system

A smart authentication system as shown in Fig. 1 was developed with colorimetric sensor array and smart cellphone. RGB images of the colorimetric sensor array were captured by Xiaomi 2S cellphone (Beijing Xiaomi Technology Co., Ltd, Beijing, China). The image settings were white balance, auto; exposure, 1/33; aperture, f/2.0; ISO, auto, and the flashlight was turned on during the photographing process. The black and white backgrounds were respectively defined as the black spots printed on the array and the white substrate. The colorimetric sensor array placed in a testing chamber. The original sensor array was captured by the smart cellphone before exposing to sample VCs. To enrich the VCs of EBN, 200 mg of EBN sample was placed in a sealed conical flask and infused with 50 mL of distilled water at 60 °C for 15 min. Then the enriched VCs from EBN infusion were pumped into the testing chamber by a vacuum pump. In this process, the smart cellphone was used to capture the image of colorimetric sensor array every one minute. It was regarded as complete equilibration when the variation ratio of RGB was less than ±2% within 5 min. Once reaching complete equilibration (about 15 min), the last image as a final image. The schematic for the identification of adulterated EBN was shown in Fig. 1.

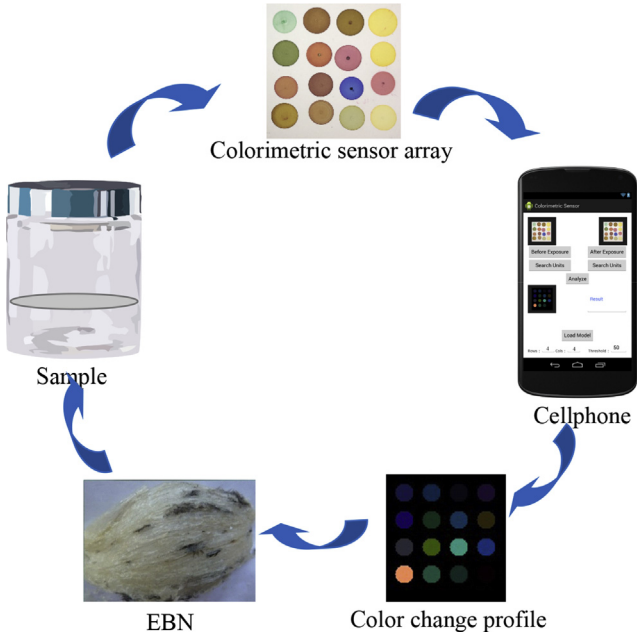

Fig. 1 – Schematic for the identification of adulterated EBN using colorimetric sensor array and smart cellphone.

2.5. Data processing and chemometric techniques

The details for the signal processing of colorimetric sensor array were present in our previous researches [16,20]. Besides, principal component analysis (PCA) was applied to reduce data dimension and illustrate the classifying trend. The hierarchical cluster analysis (HAC) was used to inquiry the similarity between authentic and adulterated EBN. Then, the back-propagation neural networks (BPNN) was used to differentiate authentic and adulterated EBN. Based on the BPNN results, partial least square (PLS) model was developed to predict the percentage of adulterates. The android app for these processing was developed using Android studio and "Android Support from Simulink" package of Matlab.

3. Results and discussion

3.1. Main nutritional components of samples

The measured percentage of the main nutritional components in different samples were present in Fig. 2. Four pure EBN, the percentage of the measured nutritional components only varied in a quite limited range. Specifically, the percentage of protein ranged from 44% to 54%, carbohydrate from 22% to 38%, Sialic acid from 80 mg/100 g to 120 mg/100 g. However, the percentage range of these components was significantly extended after the EBN samples were mixed with the mentioned adulterates. Besides, the range depended heavily on the adulterated ratio, and always covered the range of pure samples. Therefore, it is difficult to completely differentiate pure EBN and adulterated one using main nutritional components, especially for low percentage adulteration, further exploration about the VCs of EBN and adulterants was proceeded.

3.2. GC- MS detection of EBN and adulterants

The major differences between the adulterants and EBN were investigated using GC-MS. Typical GC-MS total ion current (TIC) chromatograms of EBN and adulterants were shown in Fig. 3. The volatile components with high concentration were selected as characteristic volatile components according to the GC-MS result. However, there are some special cases as Dodecane. Dodecane is the most abundant volatile component in EBN, but also appears in Egg white's volatile components with a high concentration. Therefore, the Dodecane could not be selected as a characteristic volatile components for EBN or egg white. At last, nine kinds of characteristic volatile components (Hexadecanoic acid, Propanetriol, Cyclopentane, Palmitic acid, 2,4-dimethylamphetamine, 3-methyl butyl acetate, Hydroxybutanedioic acid, Ribitol, D-sorbitol) were chosen based on the GC-MS results.

3.3. Colorimetric sensor array responses

The adulterated EBN with low percentage (10%) showed similar colorific change profiles to pure EBN. Along with the increasing of the adulterated proportion, the difference of colorific change profiles between pure EBN and adulterated

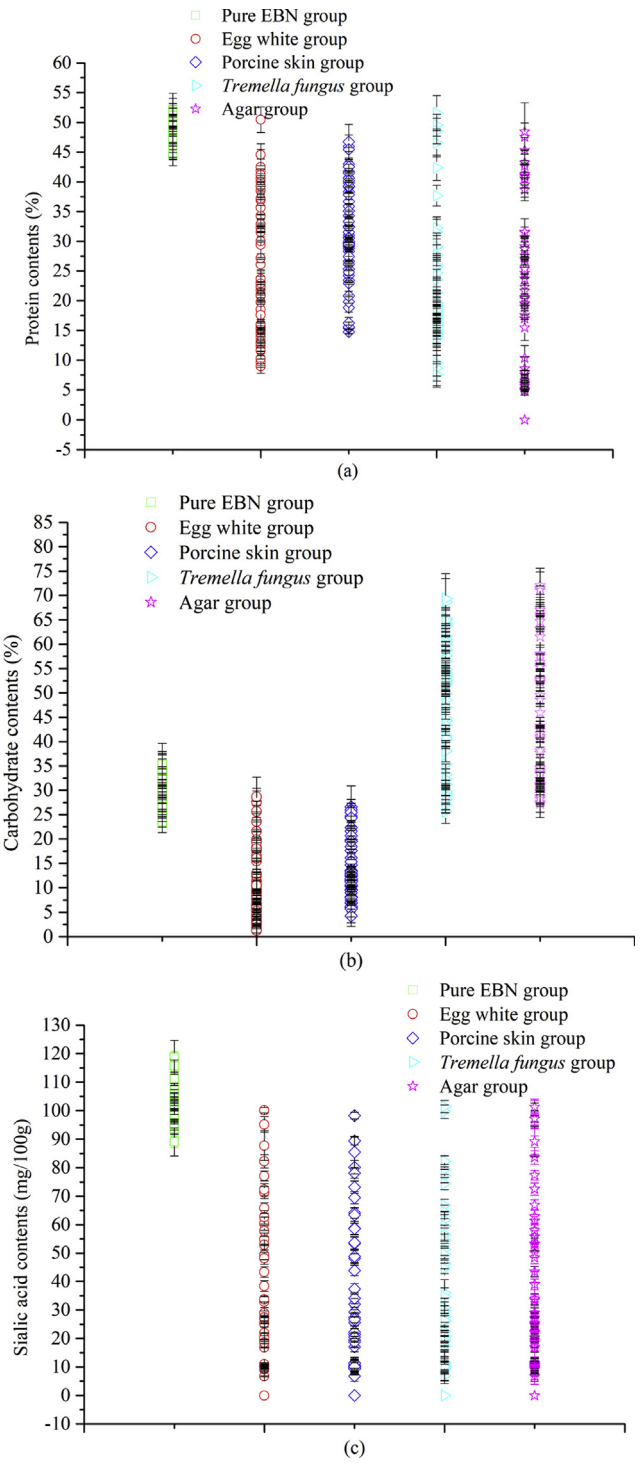

Fig. 2 – Reference values of (a) protein, (b) carbohydrate and (c) Sialic acid of pure and adulterated EBN samples measured by traditional methods.

EBN also increased. Simultaneously, differences among the adulterated samples also enlarged. In Fig. 4, different mixtures with certain adulterated proportion showed unique colorific maps by the colorimetric sensor array.

Even though pure EBN and the adulterants both contain various of VCs, colorimetric sensor array is a multi-sensor device, which not only shows cross-sensitivity but also

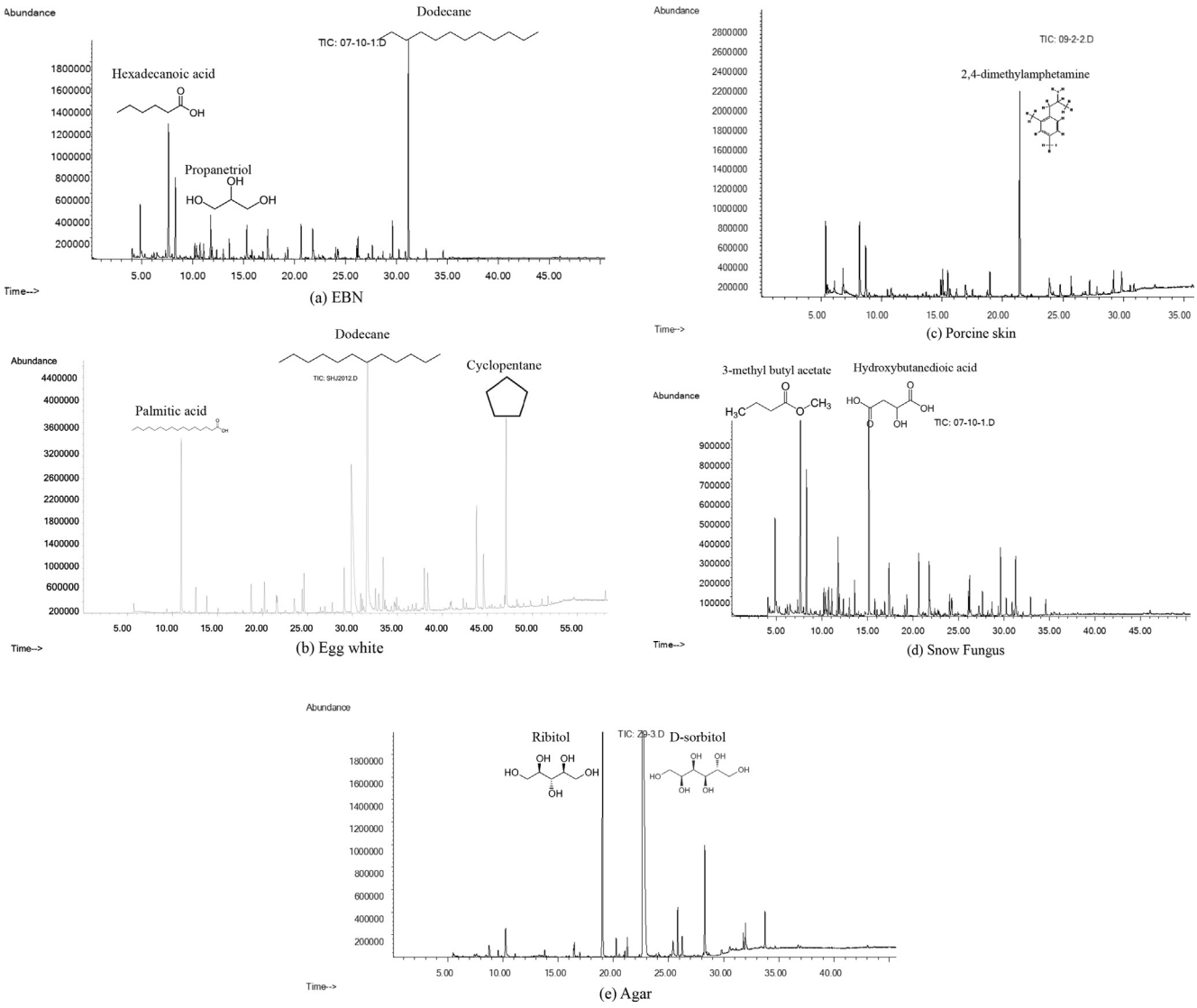

Fig. 3 – Typical GC-MS total ion current (TIC) chromatograms of EBN and adulterants.

presents high selectivity like human odor receptors. In other words, chemoresponsive dye could response to several of the VCs, and different chemoresponsive dyes could also response to the same VC. Consequently, it is difficult for colorimetric sensor array to assign specific color response to a specific VC, which differs the conventional gas composition analysis technology (e.g. GC and GC–MS). Actually, the data analysis of colorimetric sensor array is based on a black box system with the help of pattern recognition and multivariate analysis methods [26,27].

3.4. *Qualitative determination of adulteration types by PCA and HAC*

PCA and HAC were utilized to provide an overview of the capacity of the colorimetric sensor array data to characterize EBN. The first three PCs accounted for 90.23% of the total variance (PC1 = 58.42%, PC2 = 26.67%, PC3 = 5.14%). The three-dimensional score plot for the first three PCs was plotted as a scatter diagram in Fig. 5(a). The samples dispersed from the center (pure EBN) to the rim (four adulterated samples), and the higher level of adulterants contained in a mixed sample, the further distance from the pure EBN. To better visualize the differences among pure EBN, adulterated EBN and pure adulterants, HAC was performed using 30 elements with significant differences ($p < 0.05$). The measurement of the similarity was based on the squared Euclidean distance. Five sample clusters were obtain at a cut distance of 9.7 (Fig. 5(b)). Generally, the samples with the same adulterant were divided into the same cluster. To observe the relationship between pure EBN and different adulterants, the greater closeness reflecting a higher degree of sample association was also present. The HCA shows that the pure EBN samples were clustered together with egg white adulterated samples, which may be because the egg white has the most similar odor with EBN. The egg white adulterated samples were clustered together with the porcine skin adulterated samples. This result may be attributed to the reason that they are both high–protein substances. Likewise, the *tremella* fungus mixtures samples clustered together with the agar adulterated

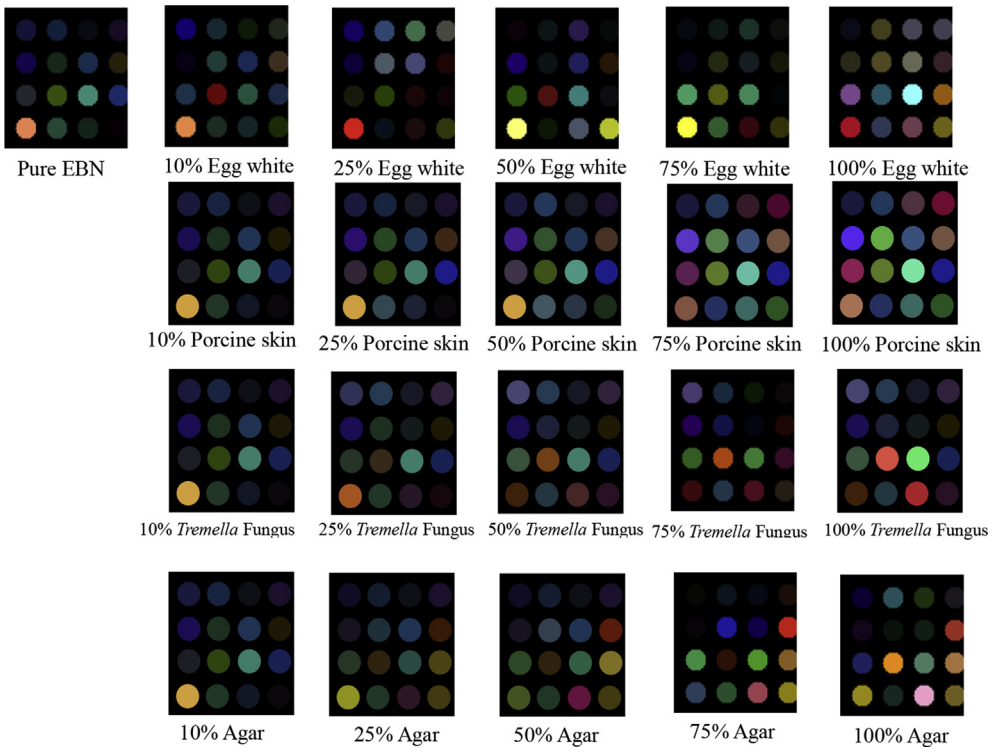

Fig. 4 – Average color change profiles of pure EBN and 4 kinds of adulterated EBN visualized as color difference maps.

samples due to the high–carbohydrate substances. The cluster results implied that multi-element information could be suitably utilized for qualitative discrimination which is consistent with the results from PCA. Both the PCA and HAC analysis illuminated the intrinsic relationship of EBN and adulteration through unsupervised learning method. It is assumed that the pattern recognition could be used to identify adulteration of EBN.

3.5. *Development multi-layered network model by BPNN and PLS*

Although the color change profiles of colorimetric sensor array could authenticate EBN and differentiate adulterated types, it is primarily based on comparisons with known samples. Therefore, it is necessary to establish a multi-layered network model to determine both the adulterated type and percentage of adulterant. Development of the multi-layered network model with back-propagation neural networks (BPNN) and partial least squares (PLS) consists of two stepwise procedures as shown in Fig. 6.

The first procedure was identification phase based on the BPNN algorithm. In this phase, only two classes need to be classified. The authentic EBN was labeled as '1', adulterated EBN as '-1'. Adulterated EBN was applied to the second procedure. The second procedure was quantification phase which included two steps, classification and prediction of adulterated percentage. In the classification step, the samples with label '-1' were identified as one of the four adulterants categories, also based on the BPNN algorithm. Prediction of adulterated percentage model were built using PLS. The details about the two stepwise procedures are followed:

3.5.1. *The identification phase*

In this phase, 1050 samples were divided into calibration and validation set. The calibration set included 120 mixtures of egg white and EBN, 120 mixtures of porcine skin and EBN, 120 mixtures of *tremella* fungus and EBN, 120 mixtures of agar and 30 pure EBN samples, 30 pure egg white samples, 30 pure porcine skin samples, 30 pure *tremella* fungus and 30 pure agar samples respectively, in total 630 samples. The other with 420 samples used as a validation set. For BPNN classification training, it is stopped at the maximum of the hyper-parameters α and β [28]. α represents the weight decay regularization, while β governs the variance of the noise. Here α and β were 3.542 and 0.435, respectively. The BPNN classification results were shown in Table 1. The recognition rates of calibration set and prediction set were 95.2% and 91.7%, respectively. The BPNN model could differentiate adulterated EBN form authentic EBN. Then the 800 adulterated EBN samples were used to further analysis.

3.5.2. *The quantification phases*

(1) step 1

All the 800 adulterated EBN samples are categorized into the four classes, marked as 'A' (pure egg white or mixture of egg white and EBN), 'B' (pure porcine skin or mixture of porcine skin and EBN), 'C' (pure *tremella* fungus or mixture of *tremella* fungus and EBN) and 'D' (pure agar or mixture of agar and EBN), respectively. Here, the discrimination of four kinds of mixtures was realized using BPNN model. For this model, the recognition rates are 93.8% and 90.6% for calibration set and prediction set, respectively, the results were shown in

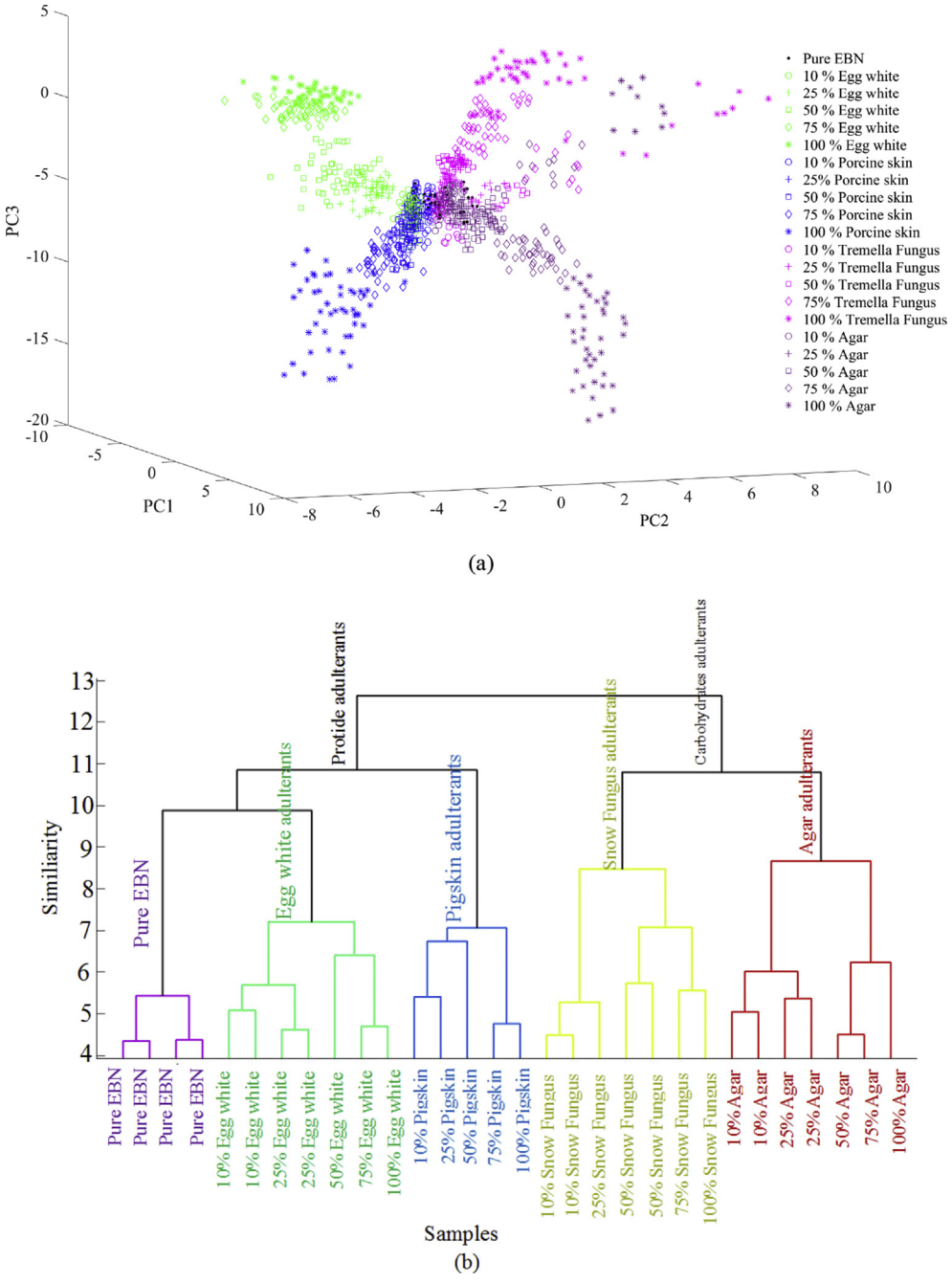

Fig. 5 – Score plots of PCA (a) and dendrogram graphs of HAC (b) based on the colorimetric array responses to pure EBN and four kinds of adulterated EBN.

Table 2. It indicates that the BPNN model could further identify the species of adulterant. However, there were a few of samples classified wrongfully. For example, three samples of the A group (egg white adulterants) were wrongly categorized as B group (porcine skin adulterants). A similar situation appeared to other groups as well. For the C group (*tremella* fungus adulterants), three samples were wrongly categorized as D group (agar adulterants). Possibly, this is because that egg white and porcine skin are high-protein substances, and porcine skin and agar are high-carbohydrates materials. The results agreed well with the HAC results.

(2) step 2

The partial least squares (PLS) regression, which is a common chemometric algorithm for multivariate analysis, was used here to establish the quantitative prediction model [29]. Four PLS model was build based on the results of step 1 corresponding to the adulterated type. The prediction error of EBN is evaluated with correlation coefficient (*R*), statistic root mean square error of calibration (*RMSEC*) and root mean square error of prediction (*RMSEP*). The *R*, *RMSEC* and *RMSEP* were calculated according to the following formulas [30]:

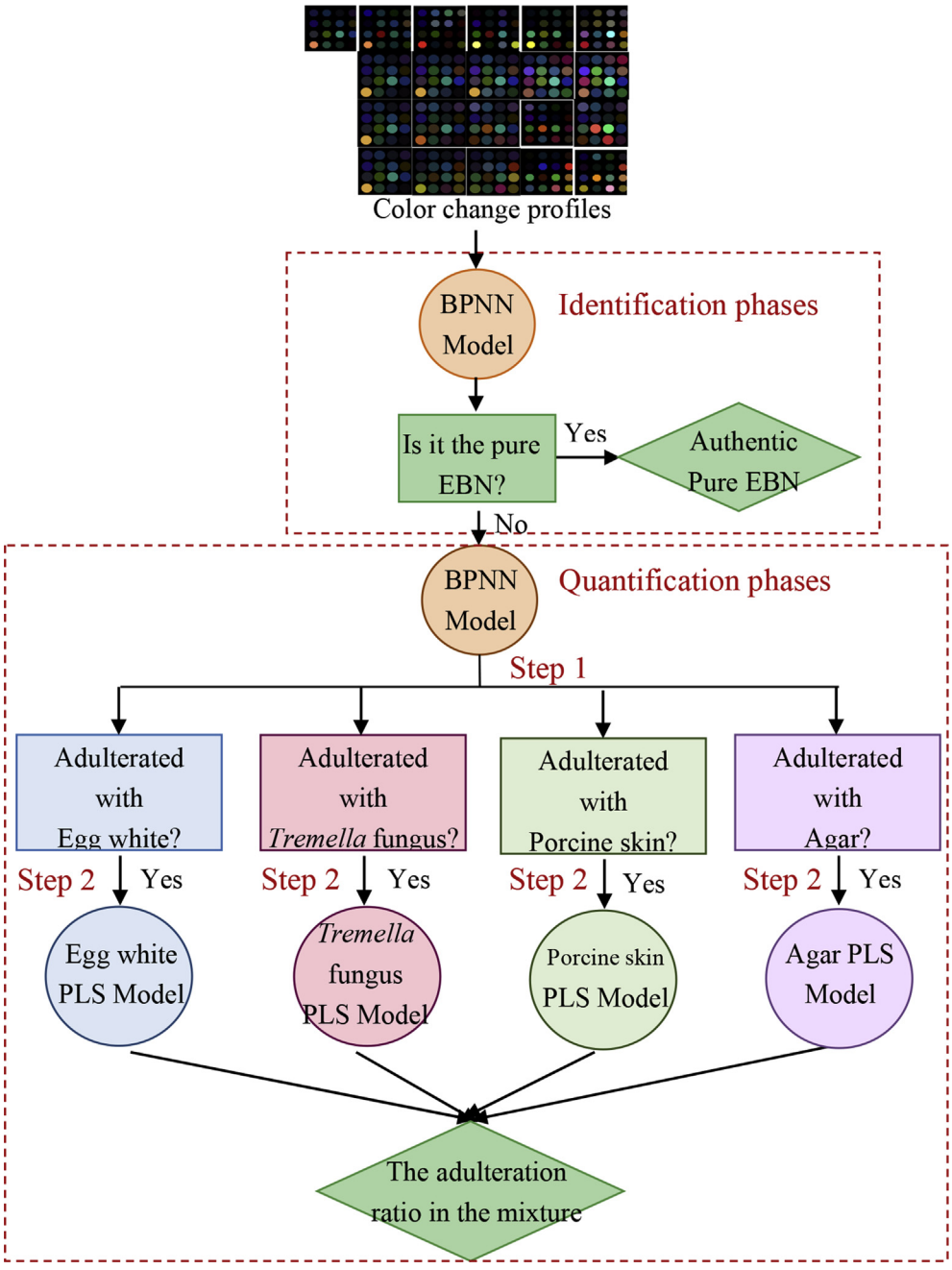

Fig. 6 – The multi-layered network model for detection and quantification of adulteration of EBN.

Table 1 – Discrimination result of authentic EBN and adulterated EBN by BPNN.

	Actual number of samples		BPNN model results		Recognition rates (%)
	Pure EBN	Adulterated EBN	Pure EBN	Adulterated EBN	
Calibration set	6	120	5	115	95.2
Prediction set	4	80	4	73	91.7

Table 2 – Discrimination result of four kinds of adulterated EBN by BPNN.

	Actual number of samples		BPNN model results				Recognition rates (%)
			A	B	C	D	
Calibration set	A	24	22	2	0	0	93.8
	B	24	1	23	0	0	
	C	24	0	0	22	2	
	D	24	0	0	1	23	
Prediction set	A	16	15	1	0	0	90.6
	B	16	2	14	0	0	
	C	16	0	0	15	1	
	D	16	0	0	2	14	

$$R = \frac{\sqrt{\sum_{i=1}^{n}(\hat{y}_i - y_i)^2}}{\sqrt{\sum_{i=1}^{n}(\hat{y}_i - \bar{y})^2}} \quad (3)$$

$$RMSECV, RMSEP = \sqrt{\frac{1}{n}\sum_{i=1}^{n}(\hat{y}_i - y_i)^2} \quad (4)$$

where, $\hat{y}_i$ is the predicted value of the ith sample, y_i is the measured value of the ith observation, n is the number of samples in the calibration or prediction set, $\bar{y}$ is the mean value of the calibration or the prediction set.

The corresponding PLS results for four individual PLS models were shown in Fig. 7. A satisfactory correlation between the colorimetric sensor array signal and the adulterant percentage was obtained, R was higher than 0.85 in both calibration and validation set. The optimized RMSECV and RMSEP for four types of adulterated EBN ranged from 0.873–0.941, which indicated that the predicted results matched well with the measured values. The colorimetric responses correlate well with those of egg white adulterant percentage, porcine skin adulterant percentage, *tremella* fungus adulterant percentage and agar adulterant percentage. Although the difference of VCs between four kinds of adulterated EBN are very subtle so that it is differentiated by the human nose with difficulty. The colorimetric sensor

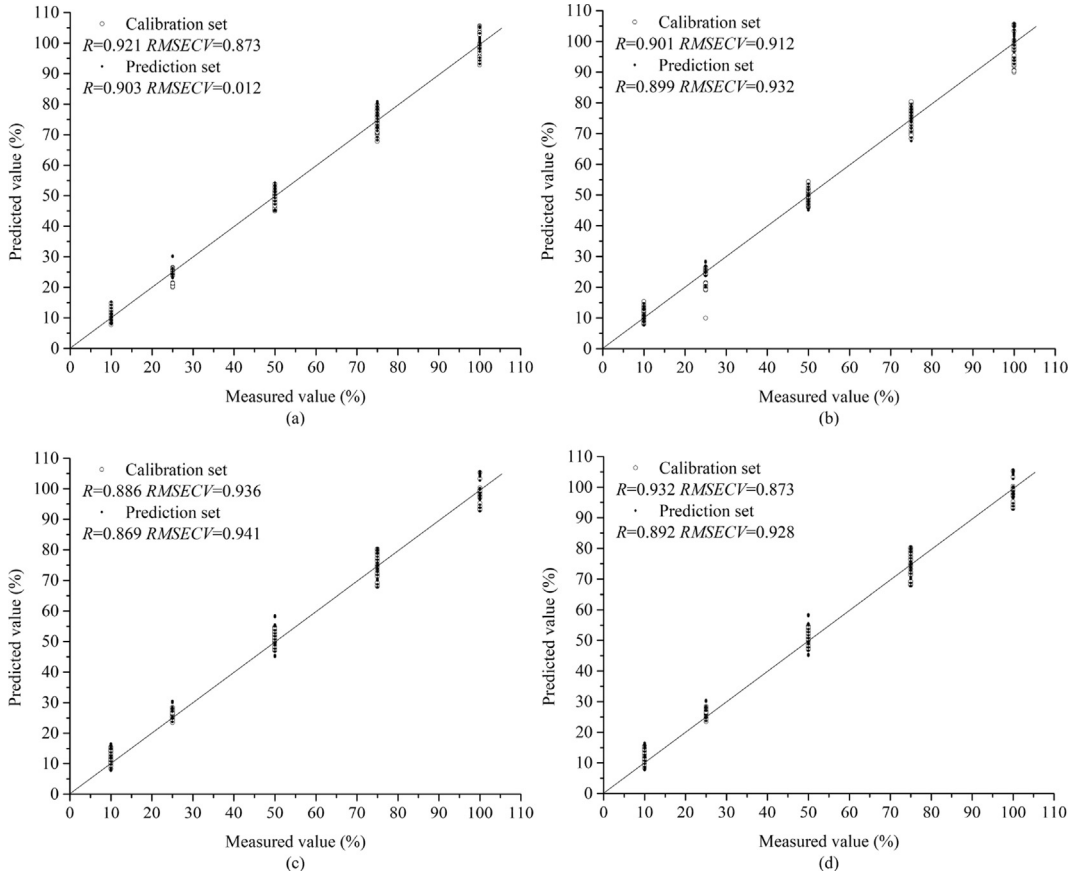

Fig. 7 – The adulterated percentage measured versus colorimetric sensor array predicted by PLS in (a) egg white adulterants, (b) porcine skin adulterants, (c) *tremella* fungus adulterants and (d) agar adulterants.

Table 3 – Identification result of test set by multi-layered network model.

Actual number of samples			Identification result						Recognition rates/Correlation coefficient
			Pure EBN	Adulterated EBN	A	B	C	D	
BPNN	Pure EBN	100	99	1	–	–	–	–	98.5%
	Adulterated EBN	100	2	98	–	–	–	–	
BPNN	A	25	–	–	23	1	0	0	92.0%
	B	25	–	–	1	23	1	0	
	C	25	–	–	0	0	23	2	
	D	25	–	–	0	1	1	23	
PLS	A	24	–	–	–	–	–	–	0.912
	B	25	–	–	–	–	–	–	0.893
	C	25	–	–	–	–	–	–	0.884
	D	25	–	–	–	–	–	–	0.909

array combined with the multi-layered network model could notice minor differences and predicte adulterated percentage.

Another 200 samples (100 pure EBN and 100 adulterated EBN) were prepared as a test set to check the effectiveness. The testing results were shown in Table 3. By using the multi-layered network models, the smart system realized the qualitative and quantitative detection of adulterated EBN. For qualitative detection, only 3 samples were misjudged by BPNN model. The 99 samples identified as adulterated EBN were further classified to four categories by BPNN model. For quantitative detection, the correlation coefficients were higher than 0.88 for the four types of adulterated EBN.

4. Conclusion

Colorimetric sensor array was developed to capture the odor information. A homebrew software based on smart cellphone was used to obtain and process the image information of colorimetric sensor array. The PCA and HAC were used to show the intrinsic relationship between the pure EBN and adulterants. The pure EBN and four types of adulterated EBN were clustered based on their volatile components. The multi-layered network model was designed for qualitative and quantitative detection of adulterated EBN. For the qualitative discrimination, the BPNN method was used to identify pure and adulterated EBN, as well as the adulterated type with a low false classification rate. For the quantitation of adulterant percentage, PLS model was developed with a high prediction accuracy. The low-cost smart system provided a real-time, nondestructive tool to authenticate EBN for customers and retailers.

Conflicts of interest

The authors declare that they have no conflict of interest.

Ethical approval

This article does not contain any studies with human participants or animals performed by any of the authors.

Informed consent

Informed consent is not applicable for the nature of this study.

Acknowledgement

This study was funded by the National Key Research and Development Program of China (2017YFC1600806); National Natural Science Foundation of China (31601543, 31801631, 31671844); Natural Science Foundation of Jiangsu Province (BK20160506, BK20180865).

REFERENCES

[1] Guo L, Wu Y, Liu M, Wang B, Ge Y, Chen Y. Authentication of edible bird's nests by TaqMan-based real-time PCR. Food Control 2014;44:220–6.
[2] Lee MS, Huang JY, Lien YY, Sheu SC. The rapid and sensitive detection of edible bird's nest (Aerodramus fuciphagus) in processed food by a loop-mediated isothermal amplification (LAMP) assay. J Food Drug Anal 2019;27(1):154–63.
[3] Lee TH, Wani WA, Koay YS, Kavita S, Tan ETT, Shreaz S. Recent advances in the identification and authentication methods of edible bird's nest. Food Res Int 2017;100:14–27.
[4] Quek MC, Chin NL, Yusof YA, Law CL, Tan SW. Pattern recognition analysis on nutritional profile and chemical composition of edible bird's nest for its origin and authentication. Int J Food Prop 2018;21(1):1680–96.
[5] Shim EKS, Chandra GF, Lee SY. Thermal analysis methods for the rapid identification and authentication of swiftlet (Aerodramus fuciphagus) edible bird's nest – a mucin glycoprotein. Food Res Int 2017;95:9–18.
[6] Guo L, Wu Y, Liu M, Ge Y, Chen Y. Rapid authentication of edible bird's nest by FTIR spectroscopy combined with chemometrics. J Sci Food Agric 2018;98(8):3057–65.
[7] Quek MC, Chin NL, Tan SW, Yusof YA, Law CL. Molecular identification of species and production origins of edible bird's nest using FINS and SYBR green I based real-time PCR. Food Control 2018;84:118–27.
[8] Quek MC, Chin NL, Yusof YA, Law CL, Tan SW. Characterization of edible bird's nest of different production, species and geographical origins using nutritional composition, physicochemical properties and antioxidant activities. Food Res Int 2018;109:35–43.

[9] Wu Y, Chen Y, Wang B, Bai L, Han WR, Ge Y, et al. Application of SYBRgreen PCR and 2DGE methods to authenticate edible bird's nest food. Food Res Int 2010;43(8):2020–6.
[10] Yang M, Cheung S-H, Li SC, Cheung H-Y. Establishment of a holistic and scientific protocol for the authentication and quality assurance of edible bird's nest. Food Chem 2014;151:271–8.
[11] Peter CYG. Authentication of Edible Bird's nest using advanced analytical techniques and multivariate data analysis. Singapore: National University of Singapore, Deparment of Chemistry; 2014.
[12] Shim EKS, Chandra GF, Pedireddy S, Lee SY. Characterization of swiftlet edible bird nest, a mucin glycoprotein, and its adulterants by Raman microspectroscopy. J Food Sci Technol 2016;53(9):3602–8.
[13] Tukiran NA, Ismail A, Mustafa S, Hamid M. Determination of porcine gelatin in edible bird's nest by competitive indirect ELISA based on anti-peptide polyclonal antibody. Food Control 2016;59:561–6.
[14] Shi J, Hu X, Zou X, Zhao J, Zhang W, Holmes M, et al. A rapid and nondestructive method to determine the distribution map of protein, carbohydrate and sialic acid on Edible bird's nest by hyper-spectral imaging and chemometrics. Food Chem 2017;229:235–41.
[15] Rakow NA, Suslick KS. A colorimetric sensor array for odour visualization. Nature 2000;406(6797):710–3.
[16] Xiao-wei H, Xiao-bo Z, Ji-yong S, Zhi-hua L, Jie-wen Z. Colorimetric sensor arrays based on chemo-responsive dyes for food odor visualization. Trends Food Sci Technol 2018;81:90–107.
[17] Jornet-Martínez N, Gómez-Ojea R, Tomás-Huercio O, Herráez-Hernández R, Campíns-Falcó P. Colorimetric determination of alcohols in spirit drinks using a reversible solid sensor. Food Control 2018;94:7–16.
[18] Lin H, Man ZX, Kang WC, Guan BB, Chen QS, Xue ZL. A novel colorimetric sensor array based on boron-dipyrromethene dyes for monitoring the storage time of rice. Food Chem 2018;268:300–6.
[19] Xiaowei H, Xiaobo Z, Jiewen Z, Jiyong S, Zhihua L, Tingting S. Monitoring the biogenic amines in Chinese traditional salted pork in jelly (Yao-meat) by colorimetric sensor array based on nine natural pigments. Int J Food Sci Technol 2015;50:203–9.
[20] Xiaowei H, Zhihua L, Xiaobo Z, Jiyong S, Hanping M, Jiewen Z, et al. Detection of meat-borne trimethylamine based on nanoporous colorimetric sensor arrays. Food Chem 2016;197:930–6.
[21] Domínguez-Aragón A, Olmedo-Martínez JA, Zaragoza-Contreras EA. Colorimetric sensor based on a poly(ortho-phenylenediamine-co-aniline) copolymer for the monitoring of tilapia (Orechromis niloticus) freshness. Sens Actuators B Chem 2018;259:170–6.
[22] Cardoso TMG, Channon RB, Adkins JA, Talhavini M, Coltro WKT, Henry CS. A paper-based colorimetric spot test for the identification of adulterated whiskeys. Chem Commun 2017;53(56):7957–60.
[23] Nogueira SA, Lemes AD, Chagas AC, Vieira ML, Talhavini M, Morais PAO, et al. Redox titration on foldable paper-based analytical devices for the visual determination of alcohol content in whiskey samples. Talanta 2019;194:363–9.
[24] Yamamoto K, Yahada A, Sasaki K, Funakoshi-Yoshida A, Ohta C, Koga N, et al. Detection of adulterated Shiikuwasha juice by sensory evaluation, colorimetric value and volatile components. Food Sci Technol Res 2013;19(5):843–8.
[25] Saengkrajang W, Matan N, Matan N. Nutritional composition of the farmed edible bird's nest (Collocalia fuciphaga) in Thailand. J Food Compos Anal 2013;31(1):41–5.
[26] Chen Q, Liu A, Zhao J, Ouyang Q. Classification of tea category using a portable electronic nose based on an odor imaging sensor array. J Pharm Biomed Anal 2013;84:77–83.
[27] Chen Q, Liu A, Zhao J, Ouyang Q, Sun Z, Huang L. Monitoring vinegar acetic fermentation using a colorimetric sensor array. Sens Actuators B Chem 2013;183:608–16.
[28] Wang Y-H, Li Y, Yang S-L, Yang L. An in silico approach for screening flavonoids as P-glycoprotein inhibitors based on a Bayesian-regularized neural network. J Comput Aided Mol Des 2005;19(3):137–47.
[29] Xiaobo Z, Jiewen Z, Povey MJW, Holmes M, Hanpin M. Variables selection methods in near-infrared spectroscopy. Anal Chim Acta 2010;667(1–2):14–32.
[30] Shmueli G, Ray S, Velasquez Estrada JM, Chatla SB. The elephant in the room: Predictive performance of PLS models. J Bus Res 2016;69(10):4552–64.